# Interplay of Flexibility and Stability in the Control of Estrogen Receptor Activity

A. Bouter, V. Le Tilly,* and O. Sire

*Laboratoire des Polymères, Propriétés aux Interfaces et Composites, Université de Bretagne-Sud, CER Yves Coppens, Campus de Tohannic, BP573, 56017 Vannes CEDEX, France*

*Received July 30, 2004; Revised Manuscript Received October 22, 2004*

ABSTRACT: Previously, we have identified an imperfect estrogen response element (*rt*ERE) in the promoter of the rainbow trout vitellogenin gene. Although this ERE leads to a lower transcriptional activation, a better estradiol stimulation in vivo as compared to consensus ERE (EREcs) was observed. Here we examine the ability of recombinant human estrogen receptor α (rhERα) to bind DNA containing the EREcs or the natural imperfect *rt*ERE, which contains three mismatches. At low salt concentration, whatever the ERE sequence, dissociation equilibrium constants of the specific rhERα−ERE complexes are similar ($K_D = 2$ nM) with the same stoichiometry. As salt concentration increases from 80 to 200 mM KCl, the affinity of the rhERα−*rt*ERE complex largely diminishes whereas that of rhERα−EREcs seems less affected. Hence the nature of the interactions stabilizing these complexes is different: more ionic in rhERα−*rt*ERE as compared to rhERα−EREcs. Moreover, kinetic measurements showed that specific rhERα−ERE complexes exhibit shorter half-lives (few seconds) and that the rhERα−EREcs complex is more stable (33 s) than the complex that formed with *rt*ERE (19.8 s), in accordance with equilibrium binding results. Finally, dynamic studies of rhERα have shown that the protein fluctuations are damped when the salt concentration increases or when bound to ERE and all the more with *rt*ERE. The interplay of affinity, complex half-lives, and protein dynamics in the transcriptional regulation of estrogen receptor is discussed.

The dynamic organization of the genome and its transcriptional regulators rule gene expression (*1*−*4*). Genes, distributed along DNA sequence, are packed into the higher-order chromatin structure (*5*) via its association with histones and other proteins as transcription factors and chaperones (*6*). Gene activation requires remodeling of chromatin and subsequent assembly of the transcriptional machinery (*7*). The complexes formed between transcription factors and chromatin are highly dynamic (*8*): transcription factors exhibit residence times on their DNA targets ranging from minutes to a few seconds (*9*), whereas the core histones remain associated with chromatin for several hours (*10*). Molecular chaperones must play a role in the dissociation of these transcriptional regulatory complexes originating the observed turnover and the ability to respond to signaling (*11*).

Estrogen receptor (ER),[1] a hormone-activated transcription factor, is involved in the regulation of genes responsible for development, growth of reproductive system, and cellular differentiation in response to hormone binding and, obviously, to its binding on target genes (*12*). In a cellular context, the majority of ER is localized in the nuclear compartment where it is trapped into transitory complexes associated with heat shock proteins; upon estradiol binding, ER molecules dissociate from these complexes and diffuse through the nucleoplasmic space until they reach response elements (*13*−*15*). Hence, in vivo, ER forms dynamic complexes with specific DNA targets of the genome and also with nuclear matrix, which can undergo rapid exchange resulting in the transcriptional responsiveness mentioned above (*4*).

ER contains six domains denoted A−F, two of which are evolutionarily conserved: the DNA-binding domain (C), DBD, with its two zinc fingers and the ligand binding domain (E), LBD, which contains a ligand-dependent activation function (AF-2). The latter contains sequences responsible for receptor dimerization (*16*−*18*) and nuclear localization (*19*). Additionally, the N-terminus, A/B domains, displays a ligand-independent activation function (AF-1) that is controlled by the phosphorylation state of the protein (*20*−*22*). D domain, a hinge region between DBD and LBD, interacts with nuclear corepressor proteins (*23*). Last, the F domain plays a role in distinguishing estrogen agonists versus antagonists (*24*). In mammals, two ER subtypes, ERα and ERβ, have been reported (*25*−*28*).

The nucleotide sequences specifically recognized by ERs are named estrogen response elements (EREs). The optimal ERE sequence consists of two six-base-pair (bp) half-sites, AGGTCA, organized as inverted repeats with a three-base-pair spacing (*29* and references therein). Upon interaction between ERE and DBD of ER, both molecules undergo conformational changes; the protein structural differences primarily concern the second zinc domain, which appears to be disordered in the free form and folded in the complexed form (*30*), whereas distortion is observed in DNA strands (*31*). Altogether these structural and flexibility changes could be critical for the differential regulation of estrogen-

* Corresponding author. Tel: 33 297 017 135. Fax: 33 297 017 071. E-mail address: letilly@univ-ubs.fr.

[1] Abbreviations: β-gal, β-galactosidase; CYC1, cytochrome *c*; DBD, DNA-binding domain; E2, 17β-estradiol; ER, estrogen receptor; ERE, estrogen response element; EREcs, consensus estrogen response element; $K_D$, dissociation equilibrium constant; LBD, ligand-binding domain; OLIns, nonspecific oligonucleotide; rhERα, recombinant human estrogen receptor α; *rt*ERα, rainbow trout estrogen receptor α; *rt*ER$_S$, N-terminal-truncated rainbow trout estrogen receptor α; *rt*ERE, rainbow trout estrogen response element; $t_{1/2}$, half-life; Vg, vitellogenin.

10.1021/bi0483716 CCC: $30.25 
Published on Web 12/16/2004

responsive genes since they likely depend on the ERE sequence to which the ER is bound.

In fish, estrogens control gonadal sex differentiation, liver vitellogenesis, and fat metabolism. The liver appears to be the most abundant organ in ER (*32*). In rainbow trout liver, estrogens up-regulate differently the expression of the estrogen receptor α (*rt*ERα) and vitellogenin (Vg) genes: higher estradiol and ERα concentrations are required for Vg gene expression (*33*, *34*). In trout liver nuclear extracts, two ERα isoforms are observed, a full-length (*rt*$ER_L$) form and an N-terminal truncation (*rt*$ER_S$) of 71 and 65 kDa, respectively. The latter *rt*ERα form, which lacks the first 41 residues present in the A-domain in other species, exhibits a significant estrogen-independent transactivation activity compared to that of *rt*$ER_L$ or human ERα (*35*). *rt*ERα and hERα exhibit a homology in amino acid sequences depending on the domains; the A/B-domain is the less conserved (20%), whereas the C-domain is the most conserved (92%) conferring a similar binding affinity (*36*).

In previous studies, we have identified the natural ERE of the *Oncorhynchus mykiss* rainbow trout vitellogenin gene (*rt*ERE) by using transient transfection assays in yeast and MCF7 cells; a single copy of this 15 bp nonpalindromic element confers estrogen-responsiveness to this gene (*37*). This natural sequence, *rt*ERE, differs from the consensus ERE, EREcs, by three mutations: GGGGCAnnnTAACCT. In transformed yeast expressing N-terminally truncated rainbow trout estrogen receptor α form (*rt*$ER_S$), we have shown that this natural imperfect ERE exhibits a lower transactivation activity but a better response to estradiol stimulation than a consensus ERE.

The aim of the present study is to quantitatively characterize the affinity, the specificity, and the stability of the complexes formed between ER and EREs. This work has been performed by using fluorescence methods. This technique allows measurement of high binding affinities (subnanomolar $K_D$) in a direct manner, study of the effects of varying physicochemical conditions such as pH, salt concentration, and temperature on the thermodynamic and kinetic parameters of the ligand-binding reactions, and observation of the protein conformational changes associated with binding. Actually, upon ligand binding, a protein conformational change may occur altering thereby the polarity of the microenvironment of the tryptophan residues, their solvent-accessibility, or both, two parameters that can be measured. In addition to these advantages, fluorescence spectroscopy brings much information on the formation of the protein−DNA complexes. In return, pure materials are required. Hence, in vitro binding experiments were performed by using pure rhERα, *rt*$ER_S$ being not yet sufficiently purified. This choice is based on the fact that, although in yeast *Saccharomyces cerevisiae* the functional activities of human and trout $ER_S$ are distinct, these two receptors exhibit a similar EREcs binding affinity (*36*). In the present study, the importance of the electrostatic properties of protein−DNA complexes in the affinity and specificity of complexes, rhERα−*rt*ERE and rhERα−EREcs, has been investigated by performing experiments at salt concentrations that better mimic the in vivo conditions. The mechanism of recognition between ER and its DNA binding sites must depend to some extent on the conformational flexibility of interacting molecules. This assumption is further supported by the observed ligand- and DNA-induced ER structural changes (*38*, *39*). Hence, to investigate the relation between (i) the structural and thermodynamic features and (ii) the dynamic behavior of ER−ERE complexes, the effect of ERE sequence on the occupancy time of rhERα on its targets and the flexibility of the bound receptor was examined. From the comparison between distinct specific rhERα−ERE complexes taking into account as a whole the thermodynamic, kinetic, and dynamic features must emerge a new framework for considering the molecular basis of transcriptional regulation.

## MATERIAL AND METHODS

### *In Vivo Study*

*Strain and Culture Media.* The *S. cerevisiae* strain used was W303.1B (α, *leu2*, *his3*, *trp1*, *ura3*, *ade2-1*, $can^R$, cyr+). Yeasts were transformed by the lithium acetate protocol (Clontech) and grown in selective medium SD/−Ura/−Leu (glucose, 20 g/L, yeast nitrogen base, 6.7 g/L, drop-out supplement without uracile and leucine, pH 5.8). For transactivation experiments, the culture medium used was YPRE (yeast extract, 10 g/L, tryptone, 20 g/L, raffinose, 5 g/L, ethanol, 3%, pH 7).

*Receptor Expression and Reporter Plasmids.* The construction of pY60*rt*er, yeast expression vector of *rt*$ER_S$ from pY60aquapo (*40*) and pCMV*rt*er (*36*) vectors was previously described (*37*).

Three reporter plasmids were used for in vivo study, YRPE2-$_1$ERE$_{cs}$, YRPE2-*rt*ERE and YRPE2-cyc (*37*). All these plasmids were derived from YRPE2 kindly provided by Prof. O'Malley. The reporter gene (*lacZ*) coding for the β-galactosidase (β-gal) was placed under the control of one sequence of EREcs (AGGTCAcagTGACCT) for YRPE2-$_1$ERE$_{cs}$ or one *rt*ERE (GGGGCAggtTAACCT) for YRPE2-*rt*ERE. ERE sequence is inserted upstream of the CYC1 promoter. For control experiments, a YRPE2-derivative plasmid without ERE sequence, YRPE2-CYC, has been constructed (*37*).

*Transactivation Assay.* Transformed yeasts were grown on selective medium (SD/−Ura/−Leu) at 30 °C until $OD_{600\ nm,l=1\ cm} = 1$ and then diluted 10 times in YPRE. Once $OD_{600\ nm,l=1\ cm} = 0.6$, the expression of the *rt*$ER_S$ was induced by adding galactose (20 g/L) with or without E2 stimulation ($10^{-8}$ and $10^{-7}$ M). β-gal activity was measured 17 h after induction with or without hormonal stimulation as previously described (*37*). All data, expressed in Miller units, are the results from at least three independent transformants.

### *In Vitro Study*

*Protein.* Full-length purified rhERα, baculovirus-expressed, was purchased from PanVera Corporation (Madison, WI) and stored at −80 °C. The protein concentration of the commercialized sample was 3 μM. One hour before every experiment, the rhERα sample was thawed and diluted to $7.5 \times 10^{-7}$ M in the assay buffer to allow protein stabilization. This sample was kept on ice for the duration of the experiments.

*Oligonucleotides.* Double-stranded oligonucleotide solutions were prepared from two 21-bp complementary oligonucleotidic sequences. These sequences were synthesized, purified, and adjusted to 100 μM by Proligo (Paris, France).

The oligonucleotide sequences of the sense strand of palindromic consensus ERE (EREcs), natural rainbow trout ERE (*rt*ERE), and nonspecific oligonucleotide (OLIns) are GTCAGGTCACAGTGACCTGAT, AGTGGGGCAGGTTAACCTAAC, and CCCACGTAAAACTGACCATCC, respectively.

The duplexes were formed by diluting each oligonucleotide in the assay buffer (Tris-HCl, 10 mM, KCl, 80 mM, pH 7.5, EDTA, 0.1 mM, DTT, 1 mM, glycerol, 10%) to obtain a final oligonucleotide concentration of 1 $\mu$M. Then both complementary oligonucleotides were mixed and heated to 85 °C for 10 min and slowly cooled to 4 °C.

For experiments requiring fluorescein-labeled oligonucleotides, only one of the strands in the duplexes was coupled to fluorescein at the 5′ end.

*Steady-State Fluorescence.* All in vitro experiments were carried out with rhERα at 10 ± 2 °C in assay buffer containing various KCl concentrations (80, 140, and 200 mM). Steady-state fluorescence emission was measured by using a SLM8100 spectrofluorimeter.

Tryptophan fluorescence spectra were obtained with bandwidths adjusted for an excitation and emission resolution of 4 and 2 nm, respectively. The excitation wavelength was 290 nm to ensure that the measured fluorescence was due to the sole tryptophanyl residues. Fluorescence emission intensity was collected with an integration time of 1 s between 300 and 430 nm. Each displayed spectrum is the average of four acquisitions.

Tryptophan fluorescence quenching experiments were achieved by using acrylamide as a quencher and monitoring protein emission in the presence of 140 mM KCl. Acrylamide is an efficient quencher of tryptophanyl fluorescence (*41*, *42*). These experiments were carried out with $3 \times 10^{-8}$ M rhERα and various acrylamide concentrations from 0 to 0.16 M. Stock acrylamide solutions (2 M) were obtained by dissolving acrylamide (Sigma) in the assay buffer.

For experiments carried out with the rhERα−EREcs complex, a EREcs concentration of $5.42 \times 10^{-8}$ M was used, whereas a *rt*ERE concentration of $8.1 \times 10^{-8}$ M was used for the rhERα−*rt*ERE complex study; in this way, at least 90% of the rhERα is specifically complexed. All experiments were repeated three times.

The quenching of fluorescence of fluorophore residues in proteins can occur in two ways: (i) static quenching arising from formation of a complex between fluorophore and quencher before excitation, (ii) dynamic quenching resulting from encounters of fluorophore and quencher molecules during the excited-state lifetime, or both. When both occur, the quenching process can be analyzed according to the modified Stern−Volmer equation:

$$\frac{F_0}{F} = (1 + K_{SV}[Q])(1 + K_a[Q])$$

where $F_0$ and $F$ represent the fluorescence intensity in the absence and in the presence of the quencher Q, respectively, and $K_{SV}$ and $K_a$ are the collisional and static quenching constants, respectively. If a single process is operating or dominating, the plot $F_0/F$ vs [Q] will be linear; if both processes occur, the plot $F_0/F$ vs [Q] will exhibit an upward curvature.

For proteins having several fluorophore residues, the quenching data can be described by the Lehrer's equation:

$$\frac{F_0}{\Delta F} = \frac{1}{f_a K_{SV}} \frac{1}{[Q]} + \frac{1}{f_a}$$

where $\Delta F = F_0 - F$ is the fluorescence intensity decrease due to the quencher concentration [Q], $f_a$ is the fractional maximum of the accessible fluorophores, and $K$ is the quenching constant. For dynamic quenching, the constant $K_{SV}$ is equal to the product $k_q\tau_0$, where $k_q$ is the bimolecular collisional rate constant and $\tau_0$ is the fluorescence decay time in the absence of quenching. The fraction of the accessible fluorophores was determined from the *y*-intercept of the plot $F_0/\Delta F$ vs 1/[Q] and the apparent quenching constant from the ratio of the *y*-intercept to the slope.

Fluorescein fluorescence anisotropy values were monitored with an excitation wavelength of 480 nm, and the bandwidth for excitation was 2 nm; the fluorescence emission intensities were collected through a 515 cutoff Oriel filter, which eliminates the excitation light scattering. The emission anisotropy, *A*, was measured according to the definition:

$$A = \frac{F_{VV} - F_{VH}(F_{HV}/F_{HH})}{F_{VV} + 2F_{VH}(F_{HV}/F_{HH})}$$

where $F_{12}$ is an emission fluorescence intensity with subscripts 1 and 2 indicating the vertical or horizontal position of the excitation and emission polarizers, respectively.

For rhERα−oligonucleotide binding titration experiments, the oligonucleotide concentration was kept constant at $5 \times 10^{-10}$ M, and the protein concentration was varied between $2 \times 10^{-10}$ and $3 \times 10^{-8}$ M. Prior to performance of measurements, the sample (oligonucleotide plus protein) was incubated for 10 min to allow protein−oligonucleotide complexation. Fluorescence anisotropy measurements were carried out with an integration time of 5 s on each emission intensity component. Data fitting was performed by nonlinear regression analysis.

For kinetic measurements of the complex dissociation, the initial value of fluorescence anisotropy of the sample containing $1 \times 10^{-9}$ M fluorescein-labeled ERE with $1 \times 10^{-8}$ M rhERα was measured after an equilibration time of 10 min. A 10-fold molar excess of unlabeled oligonucleotide was then added and quickly mixed. Data were immediately recorded with integration and interval times of 1 and 3 s, respectively. Data were fitted to single-exponential decay to obtain the dissociation rate constant.

Spectra and anisotropy values were corrected by subtracting background intensities of the buffer solution. Every displayed datum is the average of three independent experiments. Measurements were performed in a cuvette thermostated at 10 °C.

## RESULTS

*Transcriptional Activity Assay.* Recently, we have identified a nonpalindromic ERE sequence in the promoter of the rainbow trout vitellogenin gene (*37*). Transfection assays in cotransformed yeast cells with expression and reporter plasmids were used to examine the ability of *rt*ER$_S$ to activate transcription of reporter vector containing either a single

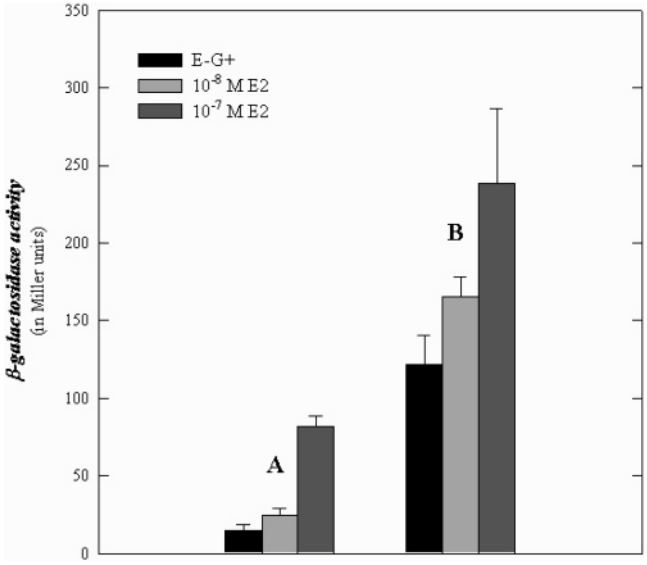


FIGURE 1: Identification of ERE in Vtg gene promoter. Yeast cells were cotransformed with the pY60rter expression vector and one YRPE2 derivative reporter plasmid: YPE2-*rt*ERE (A) and YRPE2-$_1$ERE$_{cs}$ (B). The recombinant cells were grown in YPRE medium until $OD_{600\ nm,l=1\ cm} = 0.6$ and then induced with 20 g/L of galactose. E-G+ denotes no E2 stimulation; $10^{-8}$ M E2 and $10^{-7}$ M E2 denote E2 stimulation at $10^{-8}$ and $10^{-7}$ M, respectively.

EREcs or *rt*ERE in response to E2. The effect of different E2 concentrations on *rt*ER$_S$ transcriptional activity is reported in Figure 1. For yeast cells transformed with YRPE2-$_1$ERE$_{cs}$, E2-stimulation factors of 1.4 and 2 were obtained with $10^{-8}$ and $10^{-7}$ M E2, respectively; whereas higher E2-stimulated transcription is observed from yeasts transformed with YRPE2-*rt*ERE: E2-stimulation factors of 1.6 and 5.5 were obtained with $10^{-8}$ and $10^{-7}$ M E2, respectively. No enhanced transcriptional activity was noticed with YRPE2-CYC in the presence of $10^{-7}$ M E2.

*Effect of Salt Concentration on the Affinity and the Specificity of rhERα−ERE Interaction.* The affinity of rhERα for EREcs and *rt*ERE sequences was determined by using fluorescence anisotropy methodology. Fluorescence anisotropy DNA binding curve has been already used for determining protein−DNA equilibrium (*43*−*46*). Previous studies performed at low salt concentration have reported that affinity of rhERα for ERE, either consensus or mutated motif with a single base-pair change per half-site, is roughly the same ($K_D \approx 2$ nM) with the same rhERα/ERE stoichiometry (*46*). Recently, we have reported that the rhERα binds with a nonpalindromic ERE sequence identified in the promoter of the rainbow trout vitellogenin gene; the equilibrium dissociation constant of the resulting complex is 2.5 nM at 80 mM KCl; this value is similar to that of the complex formed between rhERα and EREcs under same experimental conditions (*37*). These similar results, obtained by Szatkowski Ozers and co-workers (*46*) and us, are in opposition with current literature reporting that affinity of rhERα decreases as oligonucleotidic sequence is more degenerated (*29*). To elucidate this controversy, the effect of the salt concentration on the complex formation was investigated.

Figure 2 displays the changes of the fluorescence anisotropy value of the 5′-fluorescein-labeled oligonucleotide in the presence of increasing rhERα concentrations from $2 \times 10^{-10}$ to $3 \times 10^{-8}$ M. This latter protein concentration was limited by the concentration of the commercialized rhERα. These titration curves were obtained at 10 °C for various KCl concentrations (80, 140, and 200 mM), with both EREcs and *rt*ERE oligonucleotidic specific sequences at 0.5 nM. The effect of different salt concentrations on the interaction between rhERα and EREcs sequence is shown in Figure 2A. At 200 mM KCl, the titration curve is monophasic within the protein concentration range used, suggesting one unique protein−DNA binding equilibrium. At 80 mM KCl, the titration curve appears more complex, due to a nonspecific binding contribution observed for protein concentrations above $10^{-8}$ M. Moreover, after rhERα binding, whatever the KCl concentration, the fluorescence anisotropy value of the fluorescein-labeled oligonucleotide is roughly increased 2-fold suggesting that the stoichiometry of the rhERα−EREcs complex is not affected by an increased salt concentration (from 80 to 200 mM KCl). Besides, the titration curve is slightly shifted toward high protein concentrations as the salt concentration is increased from 80 to 200 mM. Data fitting, by using a single binding equilibrium, yields an apparent dissociation constant value of $(2.0 \pm 0.5) \times 10^{-9}$ mol·L$^{-1}$ at 80 mM KCl and $(4.8 \pm 0.7) \times 10^{-9}$ mol·L$^{-1}$ at 200 mM KCl. These values indicate that rhERα strongly binds to the EREcs sequence and that this binding is only slightly altered by salt concentration. Figure 2B displays the effect of KCl concentration on the rhERα−*rt*ERE binding titration. As above, whatever the salt concentration, we observe that the titration curve exhibits a monophasic behavior and that the fluorescence anisotropy value of the free fluorescein-labeled oligonucleotide is 2-fold lower compared to that of the complex. Though, unlike what was observed with the rhERα−EREcs complex, the titration curve is significantly shifted toward higher protein concentrations as the salt concentration is increased. Fitted data, derived from a simple binding model, yield apparent dissociation constant values of $(2.5 \pm 0.8) \times 10^{-9}$ and $(6.2 \pm 0.3) \times 10^{-9}$ mol·L$^{-1}$ at 80 and 140 mM in KCl, respectively, whereas no binding was observed at 200 mM in KCl within the rhERα concentration range used.

To assess the specificity of the rhERα−ERE interactions, titration curves were performed with OLIns. The Figure 3 displays the effect of salt concentration on the fluorescence anisotropy profile of fluorescein covalently bound to OLIns. At 80 mM KCl, the titration curve obtained with OLIns is shifted toward higher rhERα protein concentrations as compared to that obtained with EREcs or *rt*ERE sequences. In these experimental conditions, rhERα binds to OLIns with an apparent $K_D$ value of $(32 \pm 4) \times 10^{-9}$ mol·L$^{-1}$; above 80 mM KCl, no nonspecific binding was observed between $3 \times 10^{-10}$ and $3 \times 10^{-8}$ mol·L$^{-1}$ in rhERα.

Thus, the rhERα−ERE complex observed at low salt concentration, between $2 \times 10^{-10}$ and $3 \times 10^{-8}$ mol·L$^{-1}$ protein concentration range, is of course a specific complex; moreover, our data show that the interactions stabilizing this specific complex depend on the ERE sequence.

*Effect of ERE Sequence on the Kinetic Stability of the rhER−ERE Complex.* Binding equilibrium experiments have shown that the specific interaction of rhERα with the *rt*ERE sequence is highly sensitive to salt concentration in the 80−200 mM range, whereas the rhERα−EREcs specific complex was only weakly affected. Because at 140 mM KCl the dissociation equilibrium constant of both specific complexes

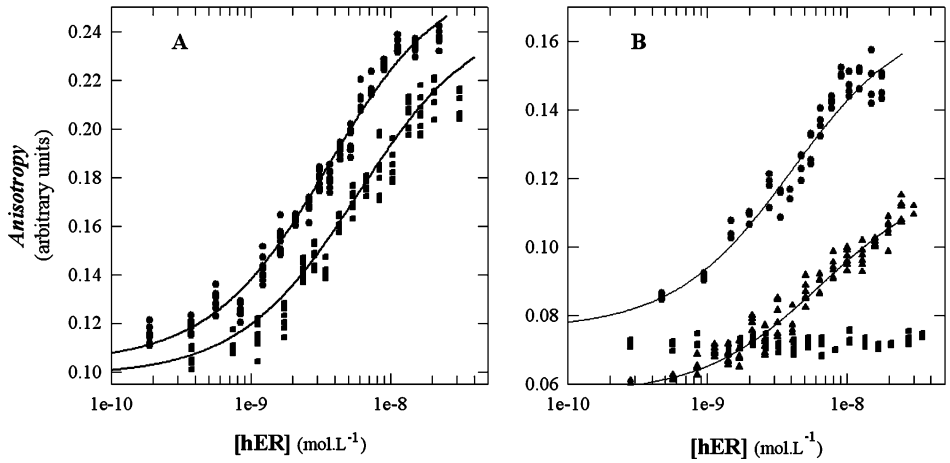


FIGURE 2: Fluorescence anisotropy profiles of 5′-fluorescein-labeled ERE upon binding with human ER: determination of apparent equilibrium constant. Titrations of $0.5 \times 10^{-9}$ mol·L$^{-1}$ labeled EREcs (A) and *rt*ERE (B) are performed at various KCl concentrations (● 80 mM, ▲ 140 mM, and ■ 200 mM). Experimental conditions are 10 mM Tris-HCl buffer, pH 7.5, 10% glycerol, 0.1 mM EDTA, 1 mM DTT at 10 °C. The lines through the data points result from data fitting using a single equilibrium model.

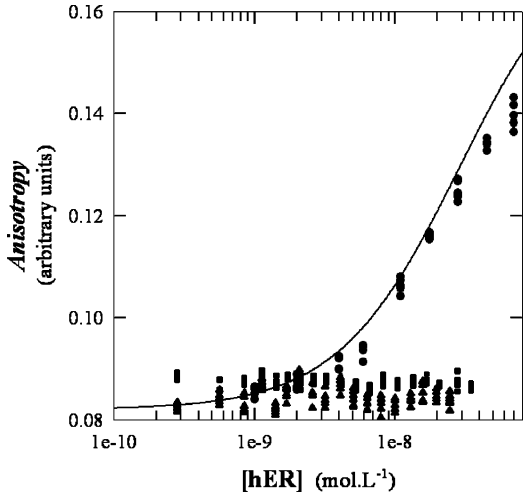


FIGURE 3: Fluorescence anisotropy profiles of the covalently bound fluorescein to a nonspecific oligonucleotidic sequence upon binding with human ER. Titrations of $0.5 \times 10^{-9}$ mol·L$^{-1}$ labeled nonspecific 21-mer are performed with three KCl concentrations: 80 (●), 140 (▲), and 200 mM (■). Experimental conditions are the same as those in Figure 2.

is at least 100-fold lower than that of the nonspecific, kinetic dissociation, studies have been performed at this salt concentration to focus on the specific complexes. The rhERα−EREcs and rhERα−*rt*ERE specific complexes were obtained by incubating fluorescein-labeled ERE at $1 \times 10^{-9}$ mol·L$^{-1}$ and rhERα at $1 \times 10^{-8}$ mol·L$^{-1}$. In these conditions, the percentage of bound oligonucleotide is about 80%. The dissociation rate of these complexes was observed, after addition of nonfluorescent oligonucleotide at $1 \times 10^{-7}$ mol·L$^{-1}$, by monitoring the fluorescein fluorescence anisotropy decrease as a function of time (Figure 4).

Figure 4A displays the time−fluorescence anisotropy change of fluorescein-labeled EREcs bound to rhERα after dilution by the same nonfluorescent ERE. The decay is best fitted by a single-exponential law, which yields a dissociation rate constant value of $(2.1 \pm 0.3) \times 10^{-2}$ s$^{-1}$. This value gives a half-life ($t_{1/2}$) for the rhERα−EREcs complex of 33 s. Figure 4B displays the time−fluorescence anisotropy decay of fluorescein-labeled *rt*ERE sequence bound to rhERα after addition of the nonfluorescent *rt*ERE. As for rhERα−EREcs dissociation, we observe a monoexponential decay of the signal. The data fitting yields a value of $(3.5 \pm 0.5) \times 10^{-2}$ s$^{-1}$ for the dissociation rate constant of specific rhERα−*rt*ERE complex; thus the $t_{1/2}$ of the rhERα−*rt*ERE complex is 19.8 s.

These results show that, in our experimental conditions, the complex $t_{1/2}$ depends on ERE sequence involved in the specific complex with a shorter $t_{1/2}$ for rhERα−*rt*ERE. These rate constant values are concordant with equilibrium binding results: at 140 mM KCl, the rhERα−EREcs complex is more stable than the rhERα−*rt*ERE.

*rhERα Flexibility at Different Salt Concentrations.* rhERα is composed of five tryptophanyl residues distributed among 595 residues in the DBD (1 tryptophan/66 residues), in the hinge region between DBD and LBD (1/64), and in the LBD (3/238). Thus, the dynamic properties of tryptophanyl residues must reflect those of the whole protein. The fluorescence properties of tryptophanyl residues of rhERα were analyzed from their averaged fluorescence lifetimes and emission spectra. No changes were observed upon KCl concentration increase from 80 to 200 mM (data not shown); the averaged fluorescence lifetime is $7.88 \pm 0.32$ ns and the wavelength of the maximum emission is 335 nm. Thus, the environment of the tryptophanyl residues of rhERα is not altered by salt concentration.

The dynamic accessibility of tryptophanyl residues in rhERα was analyzed by acrylamide as fluorescence quencher. Figure 5 displays the fluorescence emission spectra of tryptophanyl residues of rhERα (80 mM KCl) monitored at increasing concentrations of acrylamide. As acrylamide concentration increases, the fluorescence intensity decreases without noticeable change of the spectrum shape. In Figure 6A, data have been plotted according to the modified Stern−Volmer equation (see Material and Methods), $F_0/F$ vs [acrylamide], yielding a straight line between 0 and 0.16 mol·L$^{-1}$ in acrylamide; this pattern suggests that the quenching process is mainly dynamic. Besides, data were also plotted according to the Lehrer equation (see Material and Methods). From the intercept of the Lehrer plot, $F_0/\Delta F$ vs 1/[acrylamide] (Figure 6B), yielding the fraction of accessible tryptophanyl residues ($f_a$), we determined that all the five tryptophanyl residues are quenched by acrylamide. Similar

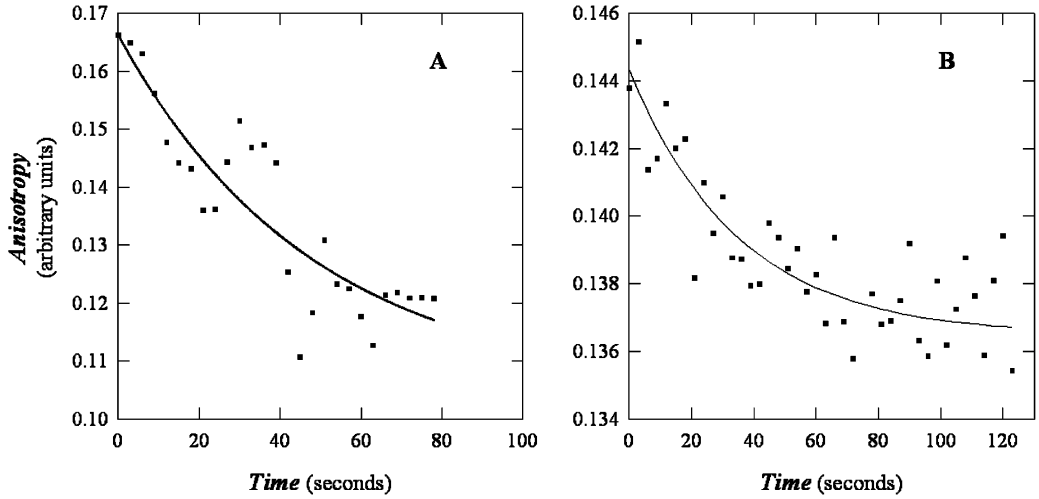


FIGURE 4: Time−fluorescence change of 5′-fluorescein-labeled ERE sequence bound to human ER after dilution by nonlabeled ERE sequence: measurement of dissociation rate constant of the specific complexes hER−EREcs (A) and hER−rtERE (B). Incubation conditions are $1 \times 10^{-9}$ mol·L$^{-1}$ fluorescein-labeled ERE with $1 \times 10^{-8}$ mol·L$^{-1}$ rhER during 15 min at 10 °C. Fluorescence anisotropy values are measured after addition of 10-fold excess of nonlabeled ERE in reaction mixture containing 140 mM KCl. The lines through the data points result from data fitting using a single-exponential function.

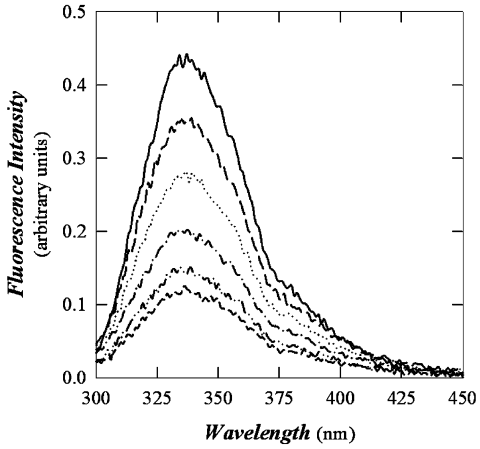


FIGURE 5: Emission spectra of the rhER tryptophan fluorescence quenched by acrylamide. The emission of $1 \times 10^{-7}$ mol·L$^{-1}$ rhER in assay buffer at 10 °C without (—) and with various acrylamide concentrations (0.025, 0.05, 0.10, 0.14, and 0.17 mol·L$^{-1}$) is monitored from 300 to 450 nm using an excitation wavelength of 290 nm. Buffer solution is composed of 10 mM Tris-HCl buffer, 80 mM KCl, pH 7.5, 10% glycerol, 0.1 mM EDTA, 1 mM DTT.

$f_a$ values of 1 were observed whatever the salt concentration; only the collisional quenching rate constants of these residues, determined from the slope of the Lehrer plot, were observed to vary with KCl concentration. As shown in Table 1, the collisional rate constant is reduced when KCl concentration increases: $11.9 \times 10^8$, $10.8 \times 10^8$, and $9.9 \times 10^8$ L·mol$^{-1}$·s$^{-1}$ for 80, 140, and 200 mM KCl, respectively. These results suggest that the dynamic accessibility of the rhERα tryptophanyl residues would decrease as the KCl concentration is increased from 80 to 200 mM. Hence at high salt concentrations, the protein would be more constrained due to lesser protein fluctuations.

*Protein Flexibility within rhERα−ERE Complexes.* Protein flexibility study within rhERα−ERE complexes has been performed with 140 mM KCl to prevent nonspecific protein−DNA complex contributions observed at 80 mM KCl. In our experimental conditions, the emission spectrum of rhERα tryptophan appears unchanged (no intensity change and no spectral shift) upon ERE binding (data not shown). This indicates that there are no $\pi-\pi$ stacking interactions between indol rings and nucleic acid bases (*47*−*49*) and that the environment of these aromatic amino acid residues seems to be not affected upon complex formation.

Whatever the specific complex, rhERα−EREcs or rhERα−*rt*ERE, the Lehrer plot yields a straight line, the intercept of which is equal to 1 (Figure 7); this result indicates that all tryptophanyl residues in the complex remain accessible to acrylamide. However, it appears that the collisional rate constant differs in the free ($10.8 \times 10^8$ L·mol$^{-1}$·s$^{-1}$) and bound states (rhERα−EREcs, $8.4 \times 10^8$ L·mol$^{-1}$·s$^{-1}$; rhERα−*rt*ERE, $7.9 \times 10^8$ L·mol$^{-1}$·s$^{-1}$): the dynamic accessibility of the tryptophanyl residues is lowered as a consequence of ER−DNA binding. Moreover, this constant also depends on the type of complex (Table 1): it is even more reduced within the complex exhibiting the lowest affinity, namely, rhERα−*rt*ERE. These results were observed to be highly reproducible since twin free- and bound-protein experiments were repeated three times: in each case, the quenching constant was lower for complexed protein as compared to the free form and lower for rhERα−*rt*ERE as compared to rhERα−EREcs.

## DISCUSSION

In vitro studies have previously reported that the estrogen receptor, with or without estrogen, specifically binds to the consensus palindromic ERE sequence, AGGTCAnnnTGACCT, as an homodimer (*50*, *51*); each subunit recognizes one half-site of the palindromic sequence. The interactions between the EREcs target and the DBD of rhERα involve direct and water-mediated protein−DNA hydrogen bonds (*30*, *52*). These water-mediated interactions confer the specificity of recognition and the stability of interaction between ERE and rhERα (*52*). In vitro, it appears that the equilibrium binding and association rate constants of the specific rhERα−EREcs complex do not depend on E2 (*46*, *53*), whereas in vivo, the transcriptional activity of rhERα depends on the presence of the hormone (*54*). Previously, it has been observed that the specific complexes formed between ER and degenerated oligonucleotidic sequences

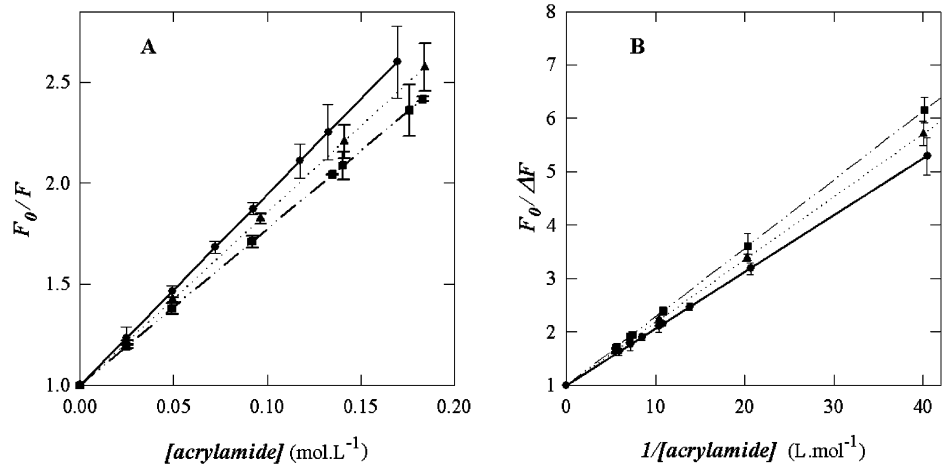


FIGURE 6: Effect of KCl concentration on rhER dynamic quenching process by acrylamide. Stern−Volmer (A) and Lehrer (B) plots of the rhER tryptophan fluorescence quenched by acrylamide are shown. Experimental conditions are the same as those in Figure 5. Buffer solution contains 80 (—), 140 (···), or 200 mM (— · —) KCl.

Table 1: rhER Fluorescence Quenching Experiments[a]

| | KCl concentration on rhER dynamics | | | ERE binding on rhER dynamics (140 mM KCl) | |
|---|---|---|---|---|---|
| | 80 mM | 140 mM | 200 mM | rhER−EREcs | rhER−*rt*ERE |
| $f_a$ | 1 | 1 | 1 | 1 | 1 |
| $K$ (L·mol$^{-1}$) | 9.4 ± 0.3 | 8.5 ± 0.2 | 7.8 ± 0.2 | 6.60 ± 0.02 | 6.2 ± 0.4 |
| $k_q$ ($10^8$ L·mol$^{-1}$·s$^{-1}$) | 11.9 | 10.8 | 9.9 | 8.4 | 7.9 |

[a] The table displays the parameters obtained from the fluorescence quenching of hER tryptophanyl residues by acrylamide. $K$ is the Stern−Volmer constant; $k_q$, the collisional rate constant between the fluorescent probe and the quencher, is calculated from $k_q = (K/\tau_0)$. $\tau_0$, the fluorescence lifetime of the hER tryptophanyl residues in the absence of acrylamide, is 7.88 ± 0.32 ns whatever the protein state, free or complexed with ERE, and whatever the salt concentration. $f_a$ is the fraction of the accessible tryptophanyl residues in hER.

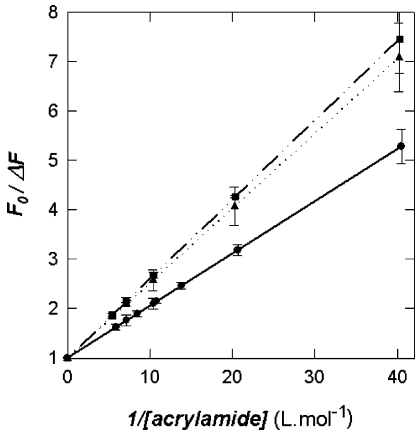


FIGURE 7: Effect of ERE binding on rhER dynamic quenching process by acrylamide. Lehrer plots of the rhER (—), rhER−EREcs (···), and rhER−*rt*ERE (— · —) tryptophan fluorescence quenched by acrylamide. Experimental conditions are the same as those in Figure 5, and the buffer solution contains 140 mM KCl.

found in most of genes in many species exhibit lower affinities as compared to the complex formed with the palindromic EREcs sequence (*29*). Recently, we have identified the natural *rt*ERE in the promoter region of the vitellogenin gene of *Oncorhynchus mykiss*; this natural sequence, a 15-bp nonpalindromic element, differs from the EREcs by three mutations: GGGGCAnnnTAACCT. As mentioned above, at low salt concentration, the binding affinity of rhERα is similar whatever the ERE sequence, EREcs or *rt*ERE. Moreover, at low salt concentration, the complexes formed between the ER and both ERE sequences exhibit two distinct stoichiometries depending on protein concentration: below $3 \times 10^{-8}$ M rhERα, the protein is bound to ERE in a 2:1 (monomer/ERE) complex, and above this concentration, higher stoichiometry is observed; the latter is observed with any OLIns sequence. The $K_D$ value of these specific complexes is about 2 nM, whereas the $K_D$ value of nonspecific complex is 15-fold higher. A similar high affinity ($K_D = 2$ nM) was yet measured at low ionic strength for the purified baculovirus-expressed human ERα binding to consensus and mutated ERE bearing a single base-pair change in each half-site (*46*) and also for purified yeast-expressed human ERα binding to consensus ERE sequence (*55*). This apparent discrepancy with the literature vanishes if one considers the effect of salts. Indeed increasing salt results in a significantly decreased affinity for the degenerated sequence, whereas the affinity for EREcs is poorly altered. The effect of an increased salt concentration is more pronounced on the complex formed with an imperfect ERE sequence as compared to the complex formed with EREcs. Similar results were already obtained with synthesized mutated ERE (*46*). These results show that one degeneracy of the ERE sequence results in a decrease of the complex affinity, which might come from a different pattern of stabilizing interactions within the complex: electrostatic interactions would dominate within the complex formed with *rt*ERE. It could be hypothesized that this particular feature allows additional modulations by charged molecules in the receptor functional nuclear compartment. Moreover, our experiments performed at 80 or 140 mM KCl show, whatever the ERE sequence (EREcs or *rt*ERE), a similar overall

anisotropy change upon rhERα binding between free and bound ERE forms; this suggests that these high-affinity complexes exhibit similar stoichiometries. The lower affinity of rhERα for *rt*ERE as compared to EREcs is concordant with its shorter $t_{1/2}$ as measured by kinetic fluorescence anisotropy. Previously, it has been shown that each base in the palindromic ERE sequence is important to retain the high affinity of the rhERα−ERE complex (*56*). Since, a bunch of experiments have assessed the relation between equilibrium binding affinity and structural features. Nevertheless, we must be aware of the preponderant role of molecular fluctuations and the resulting conformational flexibility in determining the recognition and the stabilization of protein−DNA complexes. Indeed, a low affinity associated with a short complex $t_{1/2}$ might result, among other events, in a modification of the relaxation processes, which depend on, or are of consequences for, the energy and flexibility of the interacting molecules. From the fluorescence quenching experiments presented here, it arises that all tryptophanyl residues exhibit a homogeneous dynamical accessibility whatever their protein localization. Interestingly, it is observed that both salt and ERE binding lead to restricted protein fluctuations. Hence, affinity and flexibility changes are linked since a salt concentration jump results in a decrease of both protein fluctuations and ERE affinity: the higher the protein fluctuates, the higher the affinity is. Besides, it is important to remember that the observed dynamical changes not only concern the DBD but rather reflect the overall protein conformational flexibility. Consequently, the high flexibility of rhERα observed at low salt concentration may be responsible for the poor discrimination between specific and nonspecific binding.

As a conclusion, the link between affinity and dynamics here observed allows us to propose an alternate mechanism for the various effectors involved in the fine-tuning of gene expression: any effectors altering proteins fluctuations would therefore modulate the stability and half-life of the complex, which in turn would interfere with the recruitment of subsequent transcriptional factors. Hence, the time scale of molecular interactions must have a root in the larger scale chromatin dynamics, the "fast" elementary events constituting the molecular clocks, which eventually lead to the "slow" large-scale chromatin dynamics. From this point of view, the complex half-lives would altogether be intrinsically linked to the diffusion of transcription factors toward their specific target and play a prominent role in the control of transcriptional activity. Time correlations must hence help us to a better understanding of these complex regulations.

## ACKNOWLEDGMENT

The authors are grateful to Dr. C. Royer for her help in fluorescence lifetime measurements performed on the *Plateforme RIO de Biologie Structurale* at the CBS, Montpellier, INSERM U554, CNRS-UM1 UMR 5048.

## REFERENCES

1. Chen, D., Hinkley, C. S., Henry, R. W., and Huang, S. (2002) TBP dynamics in living human cells: constitutive association of TBP with mitotic chromosomes, *Mol. Biol. Cell 13*, 276−284.
2. McNally, J. G., Muller, W. G., Walker, D., Wolford, R., and Hager, G. L. (2000) The glucocorticoid receptor: rapid exchange with regulatory sites in living cells, *Science 287*, 1262−1265.
3. Misteli, T. (2001) Protein dynamics: implications for nuclear architecture and gene expression, *Science 291*, 843−847.
4. Stenoien, D. L., Patel, K., Mancini, M. G., Dutertre, M., Smith, C. L., O'Malley, B. W., and Mancini, M. A. (2001) FRAP reveals that mobility of estrogen receptor-alpha is ligand- and proteasome-dependent, *Nat. Cell. Biol. 3*, 15−23.
5. Spector, D. L. (2003) The dynamics of chromosome organization and gene regulation. *Annu. Rev. Biochem. 72*, 573−608.
6. Jenuwein, T., and Allis, C. D. (2001) Translating the histone code, *Science 293*, 1074−1080.
7. Lemon, B., Inouye, C., King, D. S., and Tjian, R. (2001) Selectivity of chromatin-remodelling cofactors for ligand-activated transcription, *Nature 414*, 924−928.
8. Hager, G. L., Elbi, C., and Becker, M. (2002) Protein dynamics in the nuclear compartment, *Curr. Opin. Genet. Dev. 12*, 137−141.
9. Phair, R. D., and Misteli, T. (2000) High mobility of proteins in the mammalian cell nucleus, *Nature 404*, 604−609.
10. Kimura, H., and Cook, P. R. (2001) Kinetics of core histones in living human cells: little exchange of H3 and H4 and some rapid exchange of H2B, *J. Cell. Biol. 153*, 1341−1353.
11. Freeman, B. C., and Yamamoto, K. R. (2002) Disassembly of transcriptional regulatory complexes by molecular chaperones, *Science 296*, 2232−2235.
12. Mangelsdorf, D. J., Thummel, C., Beato, M., Herrlich, P., Schutz, G., Umesono, K., Blumberg, B., Kastner, P., Mark, M., and Chambon, P. (1995) The nuclear receptor superfamily: the second decade, *Cell 83*, 835−839.
13. Yamashita, S. (1998) Localization and functions of steroid hormone receptors, *Histol. Histopathol. 13*, 255−270.
14. Ylikomi, T., Wurtz, J. M., Syvala, H., Passinen, S., Pekki, A., Haverinen, M., Blauer, M., Tuohimaa, P., and Gronemeyer, H. (1998) Reappraisal of the role of heat shock proteins as regulators of steroid receptor activity,*Crit. Rev. Biochem. Mol. Biol. 33*, 437−466.
15. Stenoien, D. L., Mancini, M. G., Patel, K., Allegretto, E. A., Smith, C. L., and Mancini, M. A. (2000) Subnuclear trafficking of estrogen receptor-alpha and steroid receptor coactivator-1, *Mol. Endocrinol. 14*, 518−534.
16. Bourguet, W., Ruff, M., Chambon, P., Gronemeyer, H., and Moras, D. (1995) Crystal structure of the ligand-binding domain of the human nuclear receptor RXR-alpha, *Nature 375*, 377−382.
17. Brzozowski, A. M., Pike, A. C., Dauter, Z., Hubbard, R. E., Bonn, T., Engstrom, O., Ohman, L., Greene, G. L., Gustafsson, J. A., and Carlquist, M. (1997) Molecular basis of agonism and antagonism in the oestrogen receptor, *Nature 389*, 753−758.
18. Pike, A. C., Brzozowski, A. M., Hubbard, R. E., Bonn, T., Thorsell, A. G., Engstrom, O., Ljunggren, J., Gustafsson, J. A., and Carlquist, M. (1999) Structure of the ligand-binding domain of oestrogen receptor beta in the presence of a partial agonist and a full antagonist, *EMBO J. 18*, 4608−4618.
19. Guiochon-Mantel, A., Delabre, K., Lescop, P., and Milgrom, E. (1996) The Ernst Schering Poster Award. Intracellular traffic of steroid hormone receptors, *J. Steroid Biochem. Mol. Biol. 56*, 3−9.
20. Tzeng, D. Z., and Klinge, C. (1996) Phosphorylation of purified estradiol-liganded estrogen receptor by casein kinase II increases estrogen response element binding but does not alter ligand stability, *Biochem. Biophys. Res. Commun. 223*, 554−560.
21. Lu, Q., Surks, H. K., Ebling, H., Baur, W. E., Brown, D., Pallas, D. C., and Karas, R. H. (2003) Regulation of estrogen receptor alpha-mediated transcription by a direct interaction with protein phosphatase 2A, *J. Biol. Chem. 278*, 4639−4645.
22. Kato, S., Endoh, H., Masuhiro, Y., Kitamoto, T., Uchiyama, S., Sasaki, H., Masushige, S., Gotoh, Y., Nishida, E., and Kawashima, H. (1995) Activation of the estrogen receptor through phosphorylation by mitogen-activated protein kinase, *Science 270*, 1491−1494.
23. Kullmann, M., Schneikert, J., Moll, J., Heck, S., Zeiner, M., Gehring, U., and Cato, A. C. (1998) RAP46 is a negative regulator of glucocorticoid receptor action and hormone-induced apoptosis, *J. Biol. Chem. 273*, 14620−14625.
24. Montano, M. M., Muller, V., Trobaugh, A., and Katzenellenbogen, B. S. (1995) The carboxy-terminal F domain of the human estrogen receptor: role in the transcriptional activity of the receptor and the effectiveness of antiestrogens as estrogen antagonists, *Mol. Endocrinol. 9*, 814−825.

25. Green, S., Walter, P., Kumar, V., Krust, A., Bornert, J. M., Argos, P., and Chambon, P. (1986) Human oestrogen receptor cDNA: sequence, expression and homology to v-erb-A, *Nature 320*, 134−139.
26. Kuiper, G. G., Enmark, E., Pelto-Huikko, M., Nilsson, S., and Gustafsson, J. A. (1996) Cloning of a novel receptor expressed in rat prostate and ovary, *Proc. Natl. Acad. Sci. U.S.A. 93*, 5925−5930.
27. Flouriot, G., Brand, H., Denger, S., Metivier, R., Kos, M., Reid, G., Sonntag-Buck, V., and Gannon, F. (2000) Identification of a new isoform of the human estrogen receptor-alpha (hER-alpha) that is encoded by distinct transcripts and that is able to repress hER-alpha activation function 1, *EMBO J. 247*, 4688−4700.
28. Moore, J. T., McKee, D. D., Slentz-Kesler, K., Moore, L. B., Jones, S. A., Horne, E. L., Su, J. L., Kliewer, S. A., Lehmann, J. M., and Willson, T. M. (1998) Cloning and characterization of human estrogen receptor beta isoforms, *Biochem. Biophys. Res. Commun*. 247, 75−78.
29. Klinge, C. M. (2001) Estrogen receptor interaction with estrogen response elements, *Nucleic Acids Res. 29*, 2905−2919.
30. Schwabe, J. W., Chapman, L., Finch, J. T., and Rhodes, D. (1993) The crystal structure of the estrogen receptor DNA-binding domain bound to DNA: how receptors discriminate between their response elements, *Cell 75*, 567−578.
31. Schultz, J. R., Loven, M. A., Melvin, V. M., Edwards, D. P., and Nardulli, A. M. (2002) Differential modulation of DNA conformation by estrogen receptors alpha and beta, *J. Biol. Chem. 277*, 8702−8707.
32. Pakdel, F., Le Gac, F., Le Goff, P., and Valotaire, Y. (1990) Full-length sequence and in vitro expression of rainbow trout estrogen receptor cDNA, *Mol. Cell. Endocrinol. 71*, 195−204.
33. Flouriot, G., Pakdel, F., and Valotaire, Y. (1996) Transcriptional and posttranscriptional regulation of rainbow trout estrogen receptor and vitellogenin gene expression, *Mol. Cell. Endocrinol. 124*, 173−183.
34. Flouriot, G., Pakdel, F., Ducouret, B., Ledrean, Y., and Valotaire, Y. (1997) Differential regulation of two genes implicated in fish reproduction: vitellogenin and estrogen receptor genes, *Mol. Reprod. Dev. 48*, 317−323.
35. Pakdel, F., Metivier, R., Flouriot, G., and Valotaire, Y. (2000) Two estrogen receptor (ER) isoforms with different estrogen dependencies are generated from the trout ER gene, *Endocrinology 141*, 571−580.
36. Petit, F. G., Valotaire, Y., and Pakdel, F. (1995) Differential functional activities of rainbow trout and human estrogen receptors expressed in the yeast *Saccharomyces cerevisiae*, *Eur. J. Biochem. 233*, 584−592.
37. Bouter, A. Buisine, N., Le Tilly, V., Mouchel, N., Wolff, J., and Sire, O. submitted for publication in *Biochim. Biophys. Acta*.
38. Wood, J. R., Likhite, V. S., Loven, M. A., and Nardulli, A. M. (2001) Allosteric modulation of estrogen receptor conformation by different estrogen response elements, *Mol. Endocrinol. 15*, 1114−1126.
39. Krieg, A. J., Krieg, S. A., Ahn, B. S., and Shapiro, D. J. (2004) Interplay between estrogen response element sequence and ligands controls in vivo binding of estrogen receptor to regulated genes, *J. Biol. Chem. 279*, 5025−5034.
40. Lagree, V., Pellerin, I., Hubert, J. F., Tacnet, F., Le Caherec, F., Roudier, N., Thomas, D., Gouranton, J., and Deschamps, S. (1998) A yeast recombinant aquaporin mutant that is not expressed or mistargeted in Xenopus oocyte can be functionally analyzed in reconstituted proteoliposomes, *J. Biol. Chem. 273*, 12422−12426.
41. Eftink, M. R., and Ghiron, C. A. (1976) Exposure of tryptophanyl residues in proteins. Quantitative determination by fluorescence quenching studies, *Biochemistry 15*, 672−680.
42. Eftink, M. R., and Ghiron, C. A. (1977) Exposure of tryptophanyl residues and protein dynamics, *Biochemistry 16*, 5546−5551.
43. Jamin, N., Tilly, V. L., Zargarian, L., Besancon-Yoshpe, J., Lirsac, P. N., Gabrielsen, O. S., and Toma, F. (1996) Preliminary investigation of the interaction between the R2R3 DNA binding domain of the oncoprotein C-Myb and DNA fragments, *Int. J. Quantum Chem. 59*, 333−341.
44. LeTilly, V., and Royer, C. A. (1993) Fluorescence anisotropy assays implicate protein−protein interactions in regulating trp repressor DNA binding, *Biochemistry 32*, 7753−7758.
45. Boyer, M., Poujol, N., Margeat, E., and Royer, C. A. (2000) Quantitative characterization of the interaction between purified human estrogen receptor alpha and DNA using fluorescence anisotropy, *Nucleic Acids Res. 28*, 2494−2502.
46. Szatkowski Ozers, M., Hill, J. J., Ervin, K., Wood, J. R., Nardulli, A. M., Royer, C. A., and Gorski, J. (1997) Equilibrium binding of estrogen receptor with DNA using fluorescence anisotropy, *J. Biol. Chem. 272*, 30405−30411.
47. Lawaczeck, R., and Wagner, K. G. (1974) Stacking specificity and polarization. Comparative synopsis of affinity data, *Biopolymers 13*, 2003−2314.
48. Ishida, T., Katsuta, M., Inoue, M., Yamagata, Y., and Tomita, K. (1983) The stacking interactions in 7-methylguanine-tryptophan systems, a model study for the interaction between the 'cap' structure of mRNA and its binding protein, *Biochem. Biophys. Res. Commun. 115*, 849−854.
49. Brun, F., Toulme, J. J., and Helene, C. (1975) Interactions of aromatic residues of proteins with nucleic acids. Fluorescence studies of the binding of oligopeptides containing tryptophan and tyrosine residues to polynucleotides, *Biochemistry 14*, 558−563.
50. Sasson, S., and Notides, A. C. (1984) Inability of [$^3$H]estriol to induce maximal cooperativity of the estrogen receptor, *J. Steroid Biochem. 20*, 1027−1032.
51. Skafar, D. F., and Notides, A. C. (1985) Modulation of the estrogen receptor's affinity for DNA by estradiol, *J. Biol. Chem. 260*, 12208−12213.
52. Kosztin, D., Bishop, T. C., and Schulten, K. (1997) Binding of the estrogen receptor to DNA. The role of waters, *Biophys. J. 73*, 557−570.
53. Szatkowski Ozers, M., Hill, J. J., Ervin, K., Royer, C. A., and Gorski, J. (2001) The dissociation rate of estrogen receptor alpha from the consensus estrogen response element, *Mol. Cell. Endocrinol. 175*, 101−109.
54. Kladde, M. P., Xu, M., and Simpson, R. T. (1996) Direct study of DNA-protein interactions in repressed and active chromatin in living cells, *EMBO J. 15*, 6290−6300.
55. Carlsson, B., and Haggblad, J. (1995) Quantitative determination of DNA-binding parameters for the human estrogen receptor in a solid-phase, nonseparation assay, *Anal. Biochem. 232*, 172−179.
56. O'Lone, R., Frith, M. C., Karlsson, E. K., and Hansen, U. (2004) Genomic targets of nuclear estrogen receptors, *Mol. Endocrinol. 18*, 1859−1875.

BI0483716